

Analysis of Exposure Uniformity on Cells in Vitro with 900MHz TEM Chamber

J. N. ZHANG^a, J. X. ZHAO^a, H. M. LU^a, W. WANG^a, Z. REN^a

^a *School of Electronic Engineering, Xidian University, No. 2 South Taibai Road, Xi'an 710071, China*

Abstract

The TEM chamber is a proposed exposure device for experiments detecting cell responses to electromagnetic irradiation at the mobile frequency of 900 MHz. In this paper, we extend the traditional propagating-wave exposure to the standing-wave exposure. Four standing waves with different properties are produced respectively by two types of passive loads and two types of active loads. Systematically, the maximum E field and maximum H field of the standing waves are used to expose Petri dishes of three sizes. The standard deviation (SD) of the specific absorption rate (SAR) is calculated for the cell layer and the cell suspension. We compare the SD data to determine the best arrangement with the highest exposure uniformity while considering the exposure intensity. The investigation uses the numerical simulation of the finite-difference time-domain (FDTD) method with the result accuracy supported by comparison to theoretical data on the field distribution in the TEM chamber.

Index Terms: TEM Chamber; Exposure Uniformity; Specific Absorption Rate (SAR)

© 2011 Published by MECS Publisher. Selection and/or peer review under responsibility of the Research Association of Modern Education and Computer Science.

1. Introduction

Evaluation about electromagnetic irradiation hazards at mobile-communication frequencies depends heavily on experimental studies of exposure effects on cells in vitro. Experiments with cultured cells inherently provide accurate information of cell reactions with tight control of experimental conditions, including the cell specification, exposure intensity and uniformity, exposure duration, temperature rise, etc. The waveguide chamber and the transverse electromagnetic (TEM) chamber are two typical exposure setups commonly used in studies with cells cultured in Petri dishes or flasks [1]. Waveguide chambers are usually more preferred to the TEM chamber because they are easy to build and provide relatively larger volume of effective exposure. At the same time, the exposure efficiency is higher with the waveguide chamber than that with the TEM chamber, thus reducing the power requirement on the source. Therefore, many studies on the experimental dosimetry are focused on devices with the waveguide [2]. Studies with the TEM chamber and cultured cells are quite limited in the recent literature. However, the TEM chamber has the prominent advantage over the waveguide that the incident field of a near-uniform plane wave is produced in the sample volume. It is a general acknowledgment

that the uniformity of the incident wave plays a key role in improving the uniformity of the dosimetry [3]. Meanwhile, exposure safety guidelines, such as the ICNIRP standard, have specified the plane wave with uniform power density as the standard exposure condition for experiments at frequencies of mobile communication [4].

The specific absorption rate (SAR) in cultured cells is the dosimetry unit supporting in vitro experiments. The original SAR is provided as its distribution in exposed cells. Based on the distribution, two SAR statistics are obtained, namely, the mean and the standard deviation (SD) of the SAR. The mean SAR is a measure of the exposure intensity, which is in direct proportion to net input power of the exposure device and is easily turned to reach different exposure levels. The SAR SD is a measure of the exposure uniformity. The exposure is expected to be as much uniform as possible to increase the cell population with the same SAR and hence the same reaction. However, even the incident field is uniform, the cell container and the shaped cell culture still result in a highly nonuniform SAR distribution. In view of this, the SAR uniformity for experiments is presently required to be less than 30 % as measured by the SAR SD.

This paper intends to study the SAR uniformity by using the TEM chamber with standing-wave exposures at the mobile-communication frequency of 900 MHz. The TEM chamber is selected for reasons mentioned above. The standing waves are established by the forward and backward waves that combine into a symmetrical field distribution. With respect to the SAR uniformity in cells cultured either as a layer or a suspension, different exposure scenarios are investigated, including Petri dishes of various sizes, exposures with the maximum E field and the maximum H field, and the application of the passive load and active load. A comparison is made among SAR results and the best exposure arrangements are determined for the standing wave exposure. Further study reveals the possible improvement of the SAR uniformity by sampling at restricted area.

2. Models and Method

2.1. Exposure Setup

The geometry of the TEM chamber is shown in Fig. 1(a). The dimensions of the cross section are analytically calculated to prevent higher-order standing waves and to hold Petri dishes with diameters up to 90 mm in the available volume. The length of the TEM chamber is optimized to establish a standing wave with 4 loops from the source to the end.

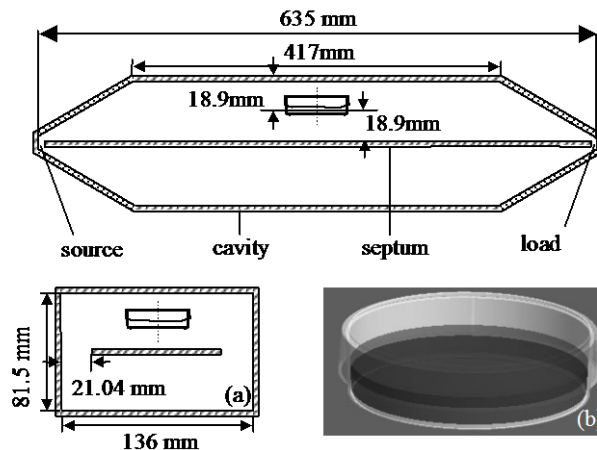


Fig. 1. The exposure setup of the TEM chamber and the Petri dish.

(a) Dimensions of the TEM chamber and the position of the Petri dish. (b) 60 mm Petri dish with the cell culture including the meniscus

Petri dishes with diameters of 35 mm, 60 mm, and 90 mm are used (Corning 430165, 430166, 430167, USA), which contain the cell culture of 3.6 ml, 11.3 ml, and 43.2 ml, respectively. Fig. 1(b) is the side view of the 60 mm Petri dish, with the meniscus surface of the cell culture considered in the model. The meniscus is established by using the profile equation in [5], with the height and decay width being 2.5 mm and 5.75 mm, respectively.

The Petri dish is placed with the main body of the liquid (that without the meniscus) at the center of the upper half space of the TEM chamber, as indicated in Fig. 1(a). The Petri dish is always E polarized, that is, the largest surface of the liquid is perpendicular to the incident E field. This orientation is not the choice to achieve the highest efficiency of the power absorption, but the field distortion by the Petri dish is the minimum. For the purpose to improve the exposure uniformity, the field distribution is the major concern.

2.2. Excitement of the Standing Wave

The source and load are set at both ends of the TEM chamber, in the gaps between the septum and the cavity. The left gap is assigned to the source with a 900 MHz sinusoidal E field and the internal resistance of 50 Ω from the cable. We have four choices for the gap on the right to establish the standing wave of different properties:

- Using the passive load of an open end to build the standing wave with the reflected wave. The E field at the middle of the TEM chamber, i.e., the position of the Petri dish, is the maximum whereas the H field is the minimum.
- Using the passive load of a short end to build the standing wave with the reflected wave. The H field at the position of the Petri dish is the maximum whereas the E field is the minimum.
- Using the active load of a source 180° off phase with the source at the left gap. The standing wave is established with two propagating waves moving in opposite directions. This arrangement also produces the maximum E field and minimum H field at the position of the Petri dish.
- Using the active load of a source in phase with the source at the left gap. The standing wave is also established with two propagating waves opposite in direction, whereas the maximum H field and minimum E field are produced at the position of the Petri dish.

The use of active loads is expected to improve the exposure uniformity since the backward wave is not the one reflected from the forward wave that is partially shielded by the Petri dish on the route.

2.3. FDTD Application

The finite-difference time-domain (FDTD) method is used to calculate the SAR distribution in cultured cells. To improve the calculation accuracy and efficiency, the chamber-dish combination is modeled with the adaptable grid. The TEM chamber is meshed with the spatial resolution of 1 mm. The voxel size is less than 1/333 of the wavelength in air so that the conformal algorithm is not necessarily used. In the volume of the Petri dish, we use the 0.2 mm mesh where the voxel size is far less than the wavelength of 39.3 mm in the cell culture as well as the skin depth of 11.6 mm. Fig. 2 shows the mesh model where the voxel size changes gradually from that of the chamber to that of the Petri dish.

In view of the symmetrical structure of the exposure setup and the symmetrical field distribution, a perfectly magnetic conductor (PMC) is inserted in the model so that only a half of the volume is virtually the problem space, as shown in Fig. 2. The symmetry boundary sets the normal E field components to zero in each step of the FDTD calculation. This approach saves half of the computer memory and nearly doubles the calculating speed. At the end of the calculation, data are symmetrically projected to the rest of the space to get the SAR distribution in the whole volume of the cell culture.

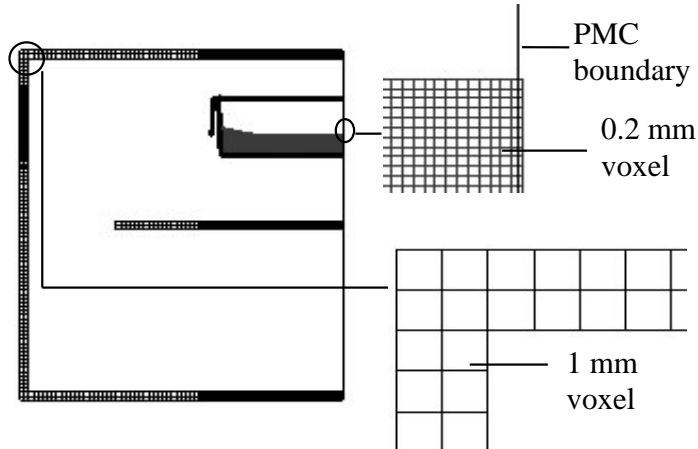


Fig. 2. Mesh model of the exposure setup and the application of the PMC as the symmetry plane to reduce the problem space to half of the original volume

Dielectric parameters of the Petri dish and cell culture are listed in TABLE I [6]. Since the parameters of cells differ very little from those of the culture medium, we use the same values for both materials. SAR statistics of the cell layer are collected on the bottom voxel layer of the cell culture. Those of the cell suspension are derived from all voxels. The mass density of cells is $1.0 \times 10^3 \text{ kg / m}^3$.

Table 1. Dielectric parameters of materials at 900 MHz and room temperature

Material	ϵ_r	$\sigma(\text{S / m})$
Cell culture	72	2.1
Petri dish	2.5	0
Air	1	0

3. Results and Discussion

3.1. Exposure Field

Fig. 3 shows the E field distributions when the standing wave is steadily established in the TEM chamber prior to the placing of the Petri dish. The FDTD results comply well with the theoretical results of the propagating wave. Without the Petri dish, the passive load of the open end and the active load of the off-phase source both generate the standing wave with the maximum E field and minimum H field at the position of the Petri dish. The exposure with the maximum H field and minimum E field is established by using the passive load of the short end or the active load of the in-phase source.

The field difference between the passive loads and active loads are shown in Fig. 4, where the 90 mm Petri dish is introduced into the TEM chamber. The large-size Petri dish is selected here to highlight the shielding effect. When the passive load of the open end is used in the exposure with the maximum E field and minimum H field, the field on the left of the Petri dish toward the source is stronger than that on the right of the dish toward the load. Fields both sides of the Petri dish are symmetrically identical with the active load of the off-phase source. Similar results are found in the exposure with the maximum H field and minimum E field.

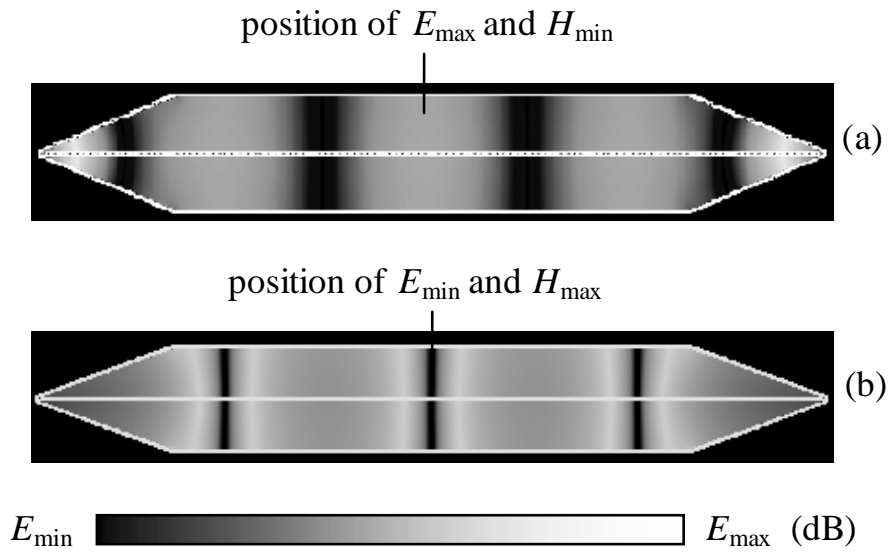


Fig. 3. E field distribution of the standing wave without the Petri dish. (a) Establishment of the maximum E field and minimum H field at the Petri dish position. (b) Establishment of the maximum H field and minimum E field at the Petri dish position

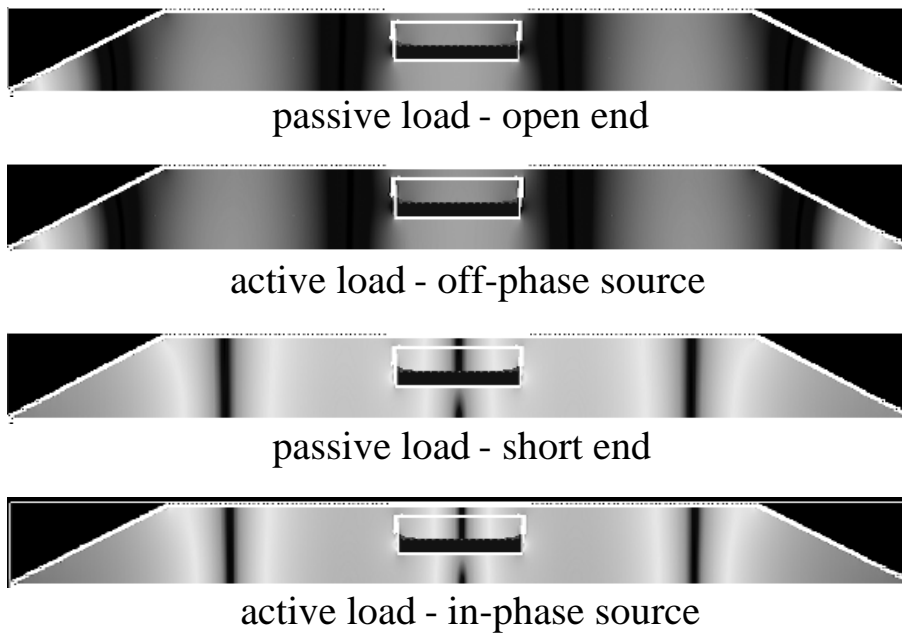


Fig. 4. Comparison between E field distributions with the 90 mm Petri dish exposed by using the passive loads and active loads

Table 2. Comparison of exposure uniformity among exposure arrangements

Exposure arrangements and the selection of the load		SAR SD (%) of the cell layer					
		35 mm Petri dish		60 mm Petri dish		90 mm Petri dish	
		Standing wave	Propagating wave	Standing wave	Propagating wave	Standing wave	Propagating wave
Exposure with E_{\max} and H_{\min}	Open end	61.46	20.54	52.24	30.10	60.73	44.36
	Off-phase source	83.42		58.73		62.45	
Exposure with H_{\max} and E_{\min}	Short end	24.31		32.17		45.71	
	In-phase source	22.53		31.54		45.62	

Exposure arrangements and the selection of the load		SAR SD (%) of the cell suspension					
		35 mm Petri dish		60 mm Petri dish		90 mm Petri dish	
		Standing wave	Propagating wave	Standing wave	Propagating wave	Standing wave	Propagating wave
Exposure with E_{\max} and H_{\min}	Open end	126.04	90.14	115.84	93.60	86.16	84.46
	Off-phase source	129.62		111.87		87.76	
Exposure with H_{\max} and E_{\min}	Short end	91.44		95.90		85.24	
	In-phase source	89.02		95.67		85.10	

3.2. Exposure Uniformity

Data of the SAR SD are listed in TABLE II for comparison among various exposure arrangements of the systematic study.

The exposure uniformity is generally better in the cell layer than that in the cell suspension. The cell suspension has a deeper dimension for the penetrating wave to vanish, therefore the SAR variance in the range is larger and the SAR SD is higher.

The active load of the source contributes to the exposure uniformity in arrangements of the H_{\max} / E_{\min} exposure. The absorption efficiency is very low with the E polarization of the Petri dish, therefore the reflected wave from the passive load is almost as strong as the excited wave from the active load. Therefore, the improvement of the exposure uniformity by using the active load is very limited.

The standing wave exposure has no obvious advantages over the propagating wave exposure in view of the exposure uniformity. However, standing waves are still the recommended choice for the TEM chamber because of the low absorption efficiency of the device and the comparable exposure uniformity of the H_{\max} / E_{\min} exposure.

3.3. Application Example

The selected exposure arrangement is the 90 mm Petri dish exposed to the H_{\max} / E_{\min} standing wave from the in-phase source. The SAR distributions in the cell layer and the cell suspension are shown in Fig. 5(a) and Fig. 5(b). The voxel counts for different levels of the SAR intensity are also given for dosimetric reference.

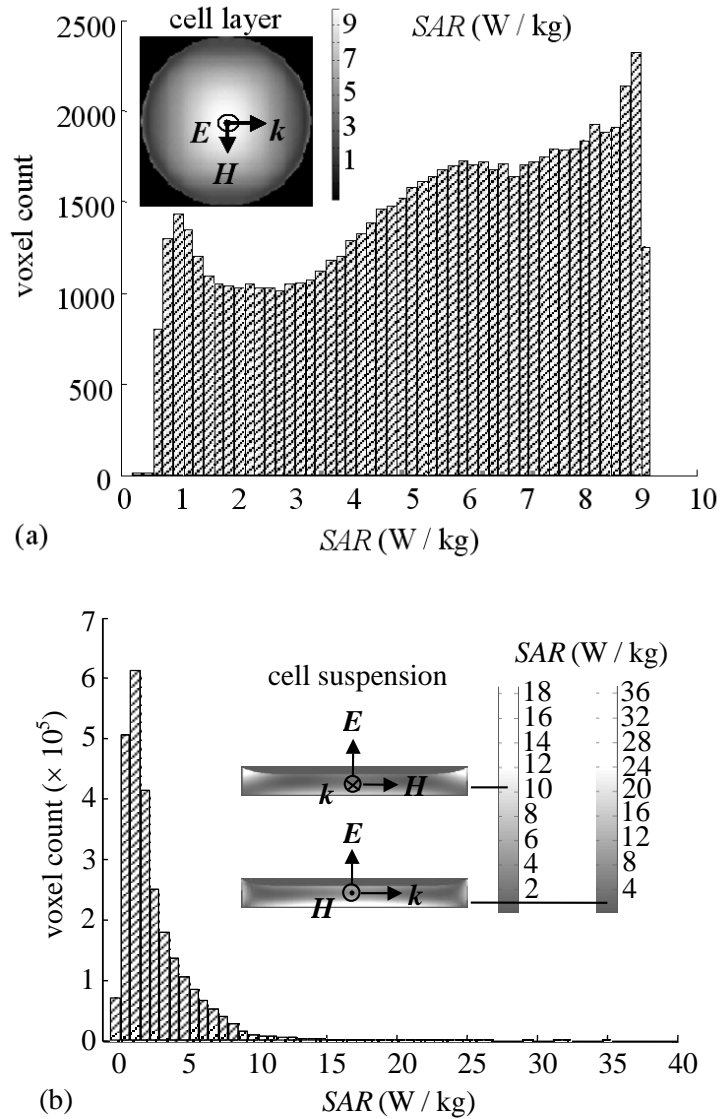


Fig. 5. Dosimetry characterizations of the selected exposure arrangement.

(a) Histogram and pattern of the SAR distribution on the cell layer. (b) Histogram and pattern of the SAR distribution in the cell suspension

Further improvements on the exposure uniformity are possible. For example, in the cell layer, the SAR uniformity is worse at the border. It is practical to restrict the sampling area toward the center to achieve higher degrees of SAR uniformity. In experiments on the cell suspension, it is observed that the meniscus contributes mostly to the SAR nonuniformity. Therefore, it is also suggested to limit the area of observation to the axis of the Petri dish. Fig. 6 shows the relation between the SAR SD and the radius of the sampling area measured from the dish axis. A sampling radius of less than 40 mm in the cell layer is found to achieve the SAR uniformity satisfying the 30 % criteria. However, due to the nonuniform SAR distribution along the axis of the Petri dish, this method is less effective for the cell suspension.

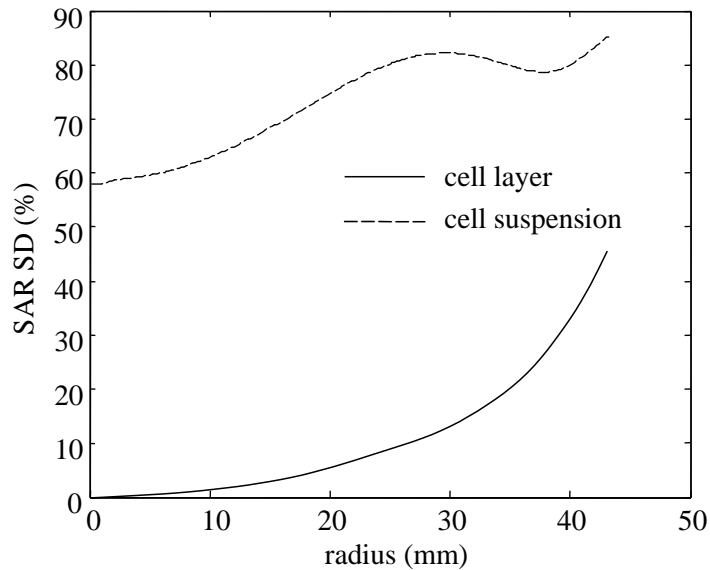


Fig. 6. Relations between the SAR SD and the radius of the sampling area in the cell layer and in the cell suspension of the selected exposure arrangement

4. Conclusion

For the 900 MHz TEM chamber and standing wave exposures, we investigated the exposure uniformity for cells cultured in the Petri dish. Different exposure arrangements are systematically compared and the best one is determined. The study is featured by the use of standing waves produced by a variety of passive and active loads, which are directly applicable to present experiments.

References

- [1] F. Schönborn, K. Poković, M. Burkhardt, and N. Kuster, "Basis for optimization of *in vitro* exposure apparatus for health hazard evaluations of mobile communications," *Bioelectromagnetics*, vol. 22, pp. 547–59.
- [2] G. Prisco, G. d'Ambrosio, M. Calabrese, R. Massa, and J. Juutilainen, "SAR and efficiency evaluation of a 900 MHz waveguide chamber for cell exposure," *Bioelectromagnetics*, vol. 29, pp. 429–438.
- [3] M. Popović, S. Hagness, and A. Taflove, "Finite-difference time-domain analysis of a complete transverse electromagnetic cell loaded with liquid biological media in culture dishes," *IEEE Trans. Bio-med. Eng.*, vol. 45, pp. 1067–1076.
- [4] ICNIRP, "Guidelines for limiting exposure to time-varying electric, magnetic, and electromagnetic fields (up to 300 GHz)," *Health Physics*, vol. 74, pp. 494–522.
- [5] J. Schuderer and N. Kuster, "Effect of the meniscus at the solid/liquid interface on the SAR distribution in Petri dishes and flasks," *Bioelectromagnetics*, vol. 24, pp. 103–108.
- [6] J. Schuderer, D. Spä, T. Samaras, W. Oesch, and N. Kuster, "In vitro exposure systems for RF exposures at 900 MHz," *IEEE Trans. Microwave Theory Tech.*, vol. 52, pp. 2067–2075.